MENGLIU
TONGLING WANG
HONGJUNZHANG
and
XUEMEI LI

# The law of metal flow during raster scribing

*The plastic forming properties of metal depend on the nature of the metal and on the deformation conditions. However, in the process of grating mechanical scribing, the flow of materials, the distribution of stress and strain fields, and the tool loading can be hardly detected and controlled. In order to obtain a better groove shape and ensure the quality of the grating geometry, the metal flow inside the material during the scratching process was studied. The equivalent strain map, stress distribution, and metal flow rate of the scratching process can be clearly obtained from the simulation results of the grating scribe, and the flow law of the metal material can be grasped. By analyzing the equivalent strain map and stress distribution of the grating scribing process, the force distribution and size of the aluminum film are obtained, which is reflected in the stress of each side of the extended pyramid knife and each blade.To provide the theoretical basis and test data for the design of diamond-like tool design and its process, so as to improve the design quality and efficiency of the tool and provide scientific basis for the orientation and development of such diamond scribe tool.*

***Keywords:*** *Metal flow, plane plastic flow, DEFORM-3D, equivalent stress distribution.*

## 1. Introduction

With the increasing application of optical components in daily life and production fields, the technology of diffraction gratings has also received increasing attention. It is well known that the performance of diffraction gratings is inextricably linked with the geometry of gratings. With the rapid development of industrial production, diffraction gratings play an extremely important role in the development of industrial science and technology. Diffraction gratings are very versatile and are widely used in spectroscopy in industrial production. A diffraction grating is a dispersive element [1], which plays a crucial role in the process of analyzing various material components and exploring the mysteries of the universe. At the same time, it is also an instrument necessary for people to develop nature. In recent years, with the rapid development of modern scientific production technology, diffraction gratings have been widely used in industrial measurement and control in various aspects. At the same time, lasers, optical communications, and integrated circuits in science and technology are also inseparable from diffraction gratings.

Mechanically scribed gratings are formed by super-precision diamond scribes on aluminum-coated glass, copper, oxygen-free copper or stainless-steel blanks (bases). It should be noted that a layer of chromium must be plated between the aluminum film and the blank substrate.This layer of chromium has a total of two functions. One of its functions is to prevent the diamond scribe from destroying the surface of the blank during the process of mechanical sculpting. At the same time, it also reduces the wear of the diamond burr; Its other function is to increase the adhesion of the glass substrate to the aluminum film through this film in order to prevent the aluminum film from falling off the glass substrate, and to have a high reflectivity over a wide spectral range. Improve the reflectivity of the grating surface. In the preparation process of the grating blank, there is a high requirement for the material of the grating substrate, and the optical glass or the Pyrex glass is generally selected. For a large-area grating, the fused silica or the chint glass should be selected. Vacuum coating for gratings also has high requirements. In the preparation of the film, vacuum distillation is used to prevent oxidation.

## 2. Basic equations of plane plastic flow

Plane plastic deformation means that the displacements of micro-elements in a denatured zone occur between parallel planes. For example, in three mutually perpendicular coordinate planes parallel to the ($x,y$) plane, all the displacements are not related to $z$.

$$\left.\begin{aligned} u_x &= u_x(x,y) \\ u_y &= u_y(x,y) \\ u_z &= 0 \end{aligned}\right\} \quad \ldots 1$$

Assuming that the material of the work piece is isotropic, the stress-strain relationship used in any plane with $z$ =

Messrs. MengLiu, HongjunZhang, Xuemei Li, College of Mechanical and Electrical Engineering, Qiqihar University, Qiqihar, China. and Tongling Wang, Department of Mechatronics, Qiqihar Institute of Engineering, Qiqihar, China.

constant is the same, and the stress component depends only on $x$ and $y$.

$$\tau_{xz} = \tau_{yz} = 0 \quad \text{... 2}$$

It can be seen that the $z$ direction is the principal axis direction, so $\sigma_z$ is the principal stress, then

$$\varepsilon_z = \gamma_{xz} = \gamma_{yz} = 0 \quad \text{... 3}$$

Or it is expressed as a component of plastic strain increments :

$$d\varepsilon_z = d\gamma_{xz} = d\gamma_{yz} = 0 \quad \text{... 4}$$

In addition,

$$\dot{\varepsilon}_z = \dot{\gamma}_{xz} = \dot{\gamma}_{yz} = 0 \quad \text{... 5}$$

If the material is incompressible, then $\varepsilon_x+\varepsilon_y+\varepsilon_z = 0$.

Thus,

$$\varepsilon_x = -\varepsilon_y \quad \text{... 6}$$

Similarly $\dot{\varepsilon}_x + \dot{\varepsilon}_y + \dot{\varepsilon}_z = 0$. And

$$\dot{\varepsilon}_x = -\dot{\varepsilon}_y \quad \text{... 7}$$

Leny-von Mises stress-strain incremental equation is

$$d\varepsilon_{ij} = \sigma'_{ij} d\lambda = \frac{3}{2}\left(\frac{d\bar{\varepsilon}}{\bar{\sigma}}\right)\sigma'_{ij} \quad \text{... 8}$$

In the formula, $\sigma_m = (\sigma_x+\sigma_y+\sigma_z)/3$

Thus,

$$\left.\begin{aligned} d\varepsilon_x &= \frac{2}{3}d\lambda\left\{\sigma_x - \frac{1}{2}(\sigma_y+\sigma_z)\right\} \\ d\varepsilon_y &= \frac{2}{3}d\lambda\left\{\sigma_y - \frac{1}{2}(\sigma_x+\sigma_z)\right\} \\ d\varepsilon_z &= \frac{2}{3}d\lambda\left\{\sigma_z - \frac{1}{2}(\sigma_y+\sigma_x)\right\} \end{aligned}\right\} \quad \text{... 9}$$

And $d\gamma_{xy} = \tau_{zy} d\gamma$

However, $d\varepsilon_z = 0$. Therefore, the third formula from equation (9)

$$\sigma_z = (\sigma_x + \sigma_y)/2 \quad \text{... 10}$$

Thus, the hydrostatic stress $\sigma_m$ can be given by

$$\sigma_m = (\sigma_x+\sigma_y+\sigma_z)/3 = \left\{\sigma_x+\sigma_y+\frac{1}{2}(\sigma_x+\sigma_y)\right\}/3 = (\sigma_x+\sigma_y)/2 \quad \text{...11}$$

Therefore, for the plane strain in the $xy$ plane, then

$$\sigma_z = \sigma_m = (\sigma_x + \sigma_y)/2 \quad \text{... 12}$$

The von Mises yield criterion is expressed as the component $\sigma_{ij}$ of the stress tensor

$$(\sigma_x - \sigma_y)^2 + (\sigma_y - \sigma_z)^2 + (\sigma_z - \sigma_x)^2 + 6(\tau^2_{xy} + \tau^2_{yz} + \tau^2_{xz}) = 6k^2$$

In the formula, $k$ is the pure shear yield stress. But for the plane strain in the $(x, y)$ plane, then $\sigma_z = (\sigma_x + \sigma_y)/2$

and $\tau_{xz} = \tau_{yz} = 0$

Therefore, $(\sigma_x - \sigma_y)^2 + (\sigma_y - (\sigma_x - \sigma_y)/1)^2 + ((\sigma_x - \sigma_y)/2$

$$- \sigma_x)^2 + 6(\tau^2_{xy} + \tau^2_{yz} + \tau^2_{xz}) = 6k^2$$

The above formula can be shortened as

$$\frac{1}{4}(\sigma_x - \sigma_y)^2 + \tau^2_{xy} = k^2 \quad \text{... 13}$$

The principal stress in the plastic deformation zone is

$$\left.\begin{aligned} \sigma_1 &= 1/2(\sigma_x+\sigma_y) + \left\{\frac{1}{4}(\sigma_x-\sigma_y)^2 + \tau^2_{xy}\right\}^{1/2} \\ \sigma_2 &= \sigma_z = (\sigma_x+\sigma_y)/2 = P \\ \sigma_3 &= 1/2(\sigma_x+\sigma_y) - \left\{\frac{1}{4}(\sigma_x-\sigma_y)^2 + \tau^2_{xy}\right\}^{1/2} \end{aligned}\right\} \quad \text{... 14}$$

The maximum principal stress in the plane of deformation can be given by

$$\tau_{\max} = k = (\sigma_1 - \sigma_3)/2 = \left\{\frac{1}{4}(\sigma_x - \sigma_y)^2 + \tau^2_{xy}\right\}^{1/2} \quad \text{... 15}$$

Thus, the principal stress can be expressed as

$$\left.\begin{aligned} \sigma_1 &= p + k \\ \sigma_2 &= \sigma_z = \sigma_m = p \\ \sigma_3 &= p - k \end{aligned}\right\} \quad \text{... 16}$$

That is, the stress state at each point in the entire plastic deformation zone can be represented by the superposition of the hydrostatic stress $p$ with the pure shear stress $k$, as shown in Fig.1. This assumes that the stress is mainly compressive in the metal forming process. Therefore, the hydrostatic stress is the compressive stress, that is, the hydrostatic pressure $p$.

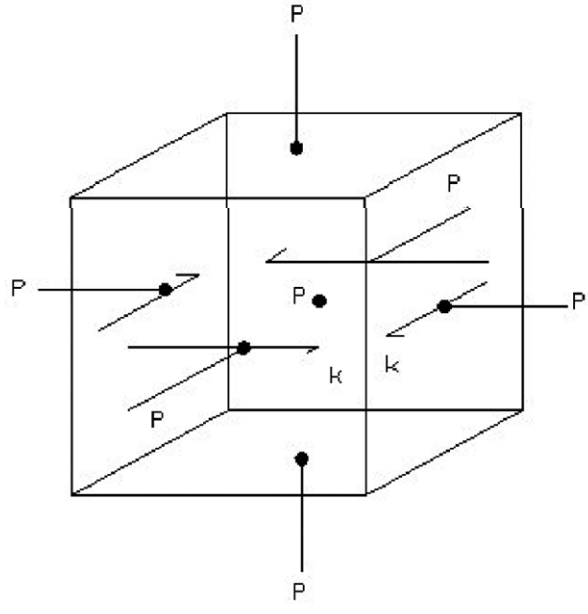


Fig.1 The stress state at one point under plane strain can be represented by the superposition of hydrostatic stress with pure shear stress

The equivalent stress or characterization stress $\bar{\sigma}$ can be given in the form of principal stress:

$$\bar{\sigma} = (1/2)^{1/2} \{(\sigma_1-\sigma_1)^2 + (\sigma_2-\sigma_3)^2 + (\sigma_3-\sigma_1)^2\}^{1/2}$$

According to the von Mises yield criterion, the above equation can be simplified as:

$$\bar{\sigma} = 3^{1/2}/2(\sigma_1-\sigma_3) = 3^{1/2}k$$

When the value of $k$ reaches $Y/2$, the yield begins. Therefore, there is no difference between the functional relationships that characterize the stress under plane strain conditions, either by the von Mises yield criterion or the Tresca yield criterion. Thus, the yield criterion can be uniformly represented by equation (13). For the von Mises yield criterion, take $k = Y/3^{1/2}$, and for Tresca yield criteria, take $k = Y/2$.

### 3. Simulation results and analysis

Deform-3D includes a preprocessor, an analog processor, and a postprocessor. Analysis of the metal plastic forming flow law mainly uses some functions of the postprocessor. The Deform-3D post-processing environment focuses on the simulation of the operation and the visualization of the results.The postprocessor is used to display the calculation result. The result can be a graphic form or a mixed form of numbers and characters. The available results are the contour lines, isokinetic maps, velocity fields, temperature fields, pressure stroke curves, etc. of the finite element mesh, equivalent stress, equivalent strain, and damage degree for each step. In addition, the user can also track points, track the trajectory, stress, strain, and damage of individual points, and extract data according to their needs.

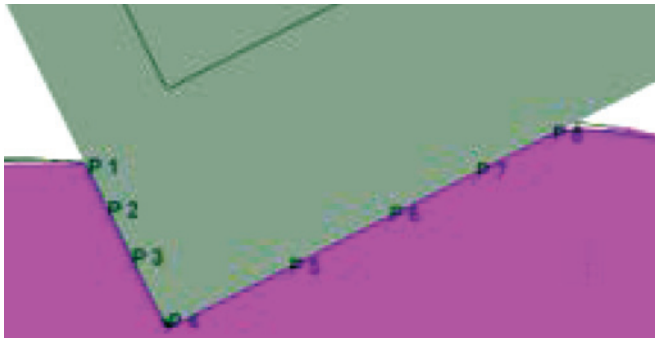

Fig.2 Horizontal point

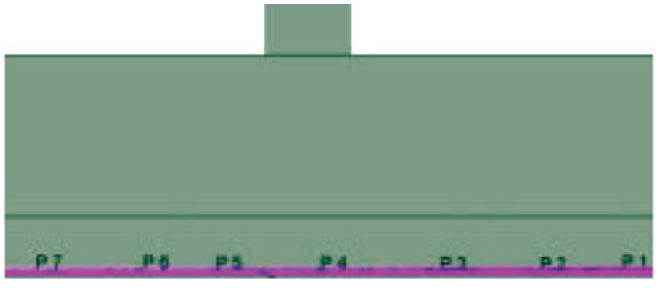

Fig.3 Vertical point

Using the functions of cloud image, contour plot and point tracking in the Deform software post-processing, the flow law of the aluminum film in the process of marking the grating was analyzed. In order to more clearly analyze the force conditions of the four surfaces of the tool and its four edges, lateral tracking points and longitudinal tracking points are respectively set. The gray part is the cutter and the pink part is the aluminum film. Lateral point tracking takes 7 points along the scribed direction, point P4 is at the tip of the tool, P1-P3 is in front of the tool nose, and P5-P7 is behind the tool nose, as shown in Fig.2. The vertical point tracking takes 8 points perpendicular to the scribe direction. Point P4 is located at the tip of the blade, P1-P3 are distributed on the flaring surface, and P5-P8 are distributed on the non-flare surface, as shown in Fig.3.

According to the result of numerical simulation in the post-processing of Deform software, the velocity vector diagram, equivalent stress diagram, and equivalent strain diagram at the time of the stable characterization of step 11580 are taken to analyze the flow state of the metal in the scoring process.

#### 3.1 Metal Flow Analysis during Scoring

In the metal plastic deformation process, the deformation speed has a great influence on the deformation.When extending the pyramid knife to grind the grating, the flow velocity of the grating aluminum film material also plays an important role in the formation process of the groove shape.I n the process of metal plastic deformation, the deformation speed of the material is expressed in terms of the degree of deformation of the material volume in a unit time. In this process, if the speed of deformation continues to increase, then the metal that has undergone cold deformation will be severely strengthened; When the deformation speed reaches a large limit and reaches the limit, the heat energy generated during the deformation process will not have time to dissipate, resulting in increased temperature of the deformed metal. Although it is not easy to control the elevated temperature, in this case it is beneficial to improve the plastic properties of the metal, and at the same time, the metal's deformation resistance is reduced, so that the plastic deformation ability of the metal is greatly improved. However, the problem to be noticed is that if the deformation speed is too high and the speed is too fast, the metal will be unevenly deformed. At the same time, the local deformation of the metal is too large and the metal is prone to cracks.

It can be seen from the velocity vector diagram in Fig.4(a) that the velocity of the metal at the position of the non-flare surface is the largest, then gradually decreases to both sides, and then the velocity becomes uniform. According to the basic law followed when the metal is plastically deformed, it can be seen that the volume does not change during metal flow. Therefore, when the tool presses the aluminum film, the extruded material bulges to the sides of

the aluminum film to form a groove. When the tool comes into contact with the aluminum film and starts to build up, the leading edge of the tool comes into contact with the aluminum film first. The material flow velocity near the aluminum film is large, and the speed direction is upward. The rest of the tool is centered on the contact part and expands in a fan-shaped manner. With the increase of the degree of metal deformation, the shape of the groove is gradually formed, the area where the material flow velocity is greater is also larger, and the flow speed of the material is declining outward from the top of the groove.

According to the law of least resistance [37], in the process of plastic deformation, the material flows in the free space. If the metal point has the possibility of moving in several directions, the metal always moves in the direction with the least resistance. The minimum resistance law conforms to the general principle of mechanics, and it is one of the most basic laws in plastic forming processing. This is the basis for judging the plastic flow direction of the mass in the deformed body. By changing the flow resistance in a certain direction, the amount of metal flow in certain directions can be changed so as to form a proper shape and eliminate defects, so that a better groove shape quality can be obtained. Therefore, the speed of the area travelled by the tool is parallel to the groove shape. When the cutting edge passes through the aluminum film, a vortex area appears at the tip speed. The 1/4 velocity from both sides of the plate is vortexed toward the tool tip, and the rest of the plate is uniformly and steadily upward.However, the minimum resistance law can only be used to roughly determine the macroscopic plastic flow conditions. In fact, the displacement direction of the particles is not always the direction of the least resistance. The direction in which the extensional strain increase is largest corresponds to the direction in which the stress generation value is maximum (i.e., the minimum resistance), but due to the integrity of the deformation, the direction in which the extensional strain increase is maximal does not correspond to the direction of the particle displacement.

According to the further analysis of the lateral point tracking speed diagram in Fig.4(b), it can be seen that the maximum speed is point P7, and the P5 point located below the tool front edge and the P1 point located on the back edge are also very fast. Therefore, the maximum speed distribution area is at the tool nose and the lower edge of the front edge; From the velocity plot of the vertical point trace in Fig.4(c), it can be seen that the maximum velocity

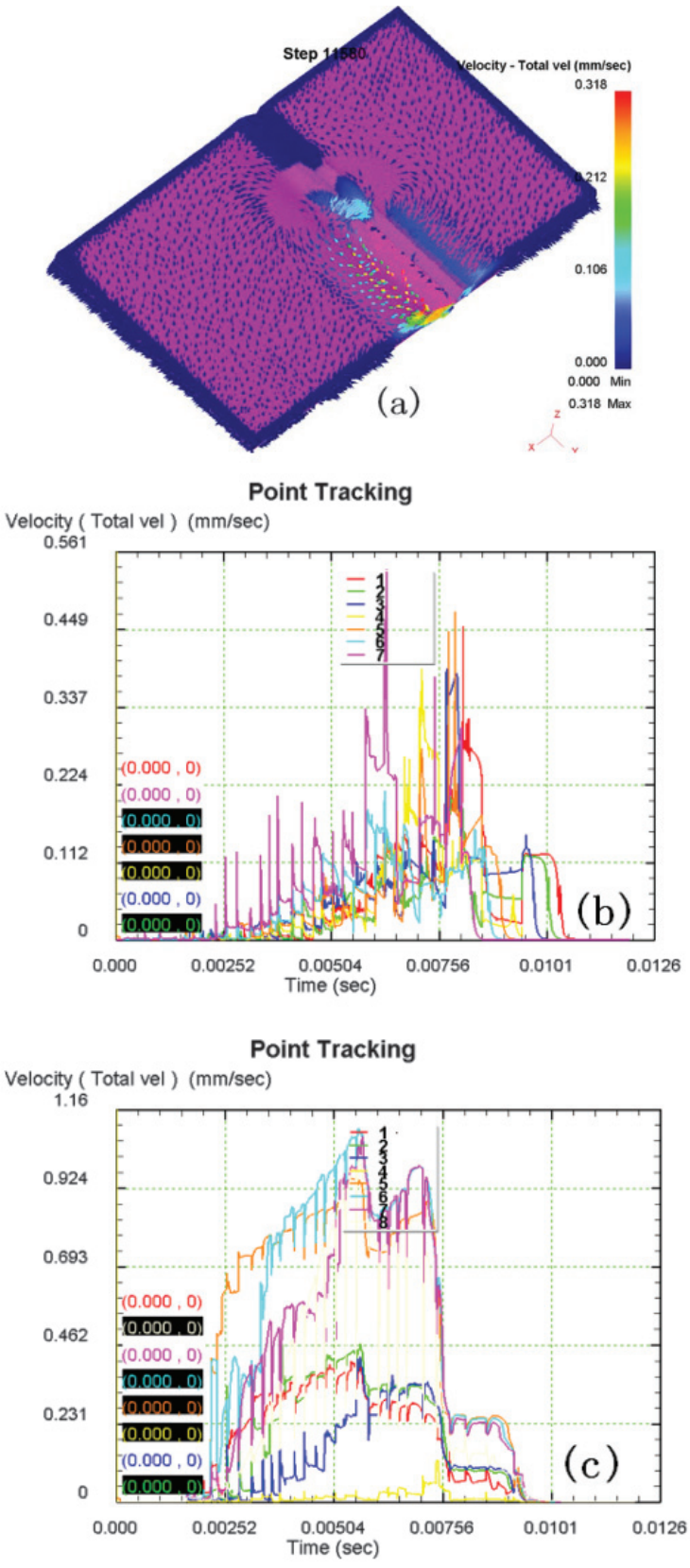


Fig.4 Speed diagram

(a) Speed vector (b) Lateral point tracking speed diagram (c) Vertical point tracking speed diagram

occurs on the non-flare P6 point, and the P5-P8 points on the non-flare surface are significantly faster than the P1-P3 on the flare surface. Therefore, the analysis of the three velocity diagrams can be concluded that the material flow in the lower area of the front edge and the non-flare surface of the tool is more severe during the process of grating the grating.

### 3.2 Equivalent Stress Distribution

The object is affected by various factors in the outside world, such as force, temperature field, etc. In the case of deformation under these conditions, various factors are generated due to resistance to the outside world.Therefore, an internal force will be generated between the various parts of the object itself, and this force will try to restore the deformed object to its original shape, that is, the ability to return the object from the position of the deformed shape to the position before the deformation. At this point, we will intercept a fixed interface to investigate the force of the object, and finally we get the internal force on a unit area is called the stress. Stress is the force generated by a structure's resistance to a load and is an important indicator of whether a product's structure is damaged (damaged) or not.The applied load acts together and the interior of the structure creates resistance, that is, stress.

In general, the shape of the structure is very complicated. According to the type of applied load, the stress is not the same, there are various stresses such as large stress, small stress, compressive stress, and tensile stress.According to the theoretical research of the metal deformation scholars and various experimental studies, we can conclude that there is a tri-axial stress in an object. The more the number of compressive stresses present in a stress species, the better the plastic properties of the object. If the number of tensile stresses present in the stress species in this object is greater, then the plastic properties of the object will be worse. In industrial production, therefore, the influence of the stress state of the object on the plastic deformation of the metal should be taken into account in the process of selecting the plastic forming process.

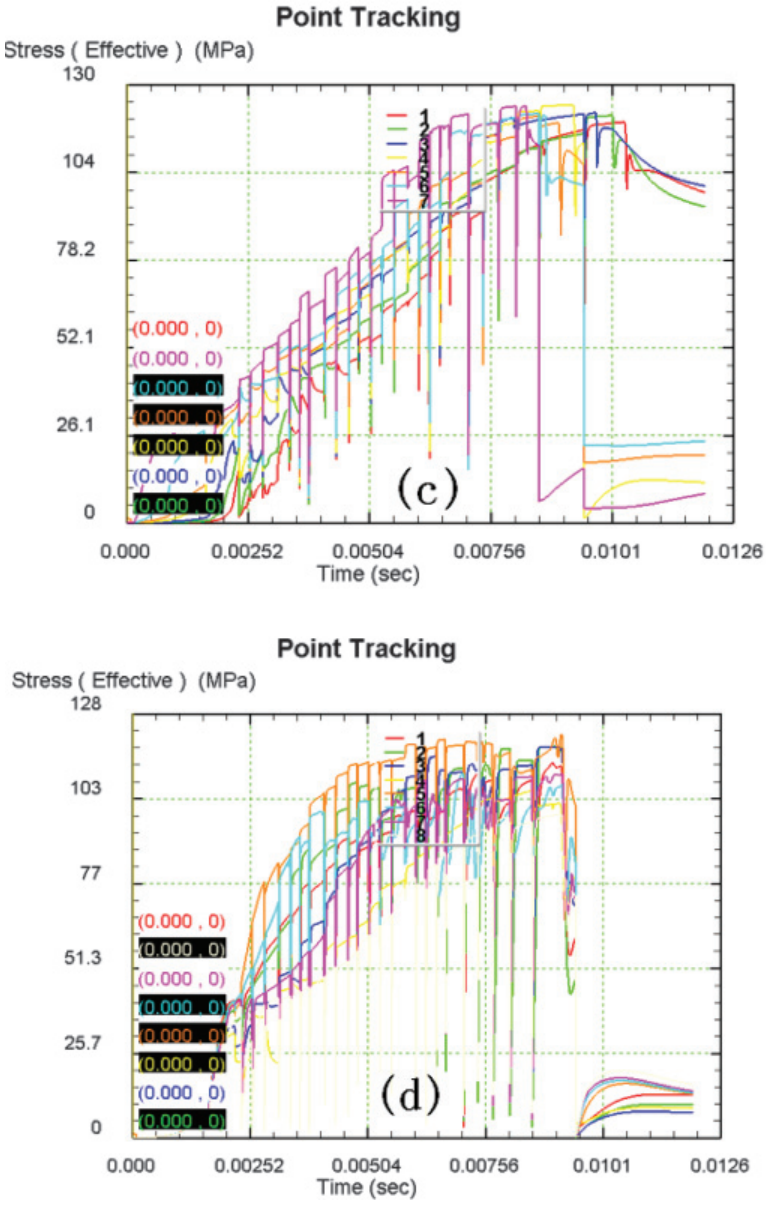


Fig.5 Equivalent stress diagram

(c) Lateral point tracking stress diagram (d) Longitudinal point tracking stress diagram

According to the size of the load, it can be seen that if the stress is large, the object must be damaged. Therefore, the stress cannot be designed to exceed a certain value. For this reason, it is necessary to know the value of stress before designing. The magnitude of the stress is important to determine whether the product and the structure are damaged. Even if the product is not damaged, the function and performance of the product are damaged because of excessive deformation. Therefore, it is particularly important to use the results of deformation for stress analysis during raster scribing.

Fig.5 shows the distribution of equivalent stress in the metal plastic deformation zone. the equivalent stress cloud can be seen from the figure that the stress of the flaring plane and the non-flare plane are compared during the squeezing and pressing process. concentrated. With the knife edge as the boundary, the maximum stress area is distributed in the area where the tool tip is not before the tool tip.The magnitude of force decreases from the point where the tool is engraved to the outside of the aluminum film. For the grating aluminum film, as the deformation increases, the expansion

range becomes larger and larger, and the bottom of the groove is the main force area. At this time, it should be noted that the stress at the bottom of the groove should be lower than the ultimate stress of the aluminum film. At the same time, it should be noted that in the process of deformation, the internal stress of the material is not uniform, and the material will cause local increase of the stress due to the change of the interface size, resulting in stress concentration. Therefore, when designing the tool, pay attention to the force of the tool tip. From the distribution area of the isoline, the maximum stress distribution area shines more than the non-flare surface.

According to the results of lateral point tracking in Fig.5(c), it can be seen that the maximum stress occurs at point P7 in front of the tool nose, and the stress value at point P4 at the tool tip is also large. At the same time, the stress values at points P2 and P3 below the leading edge of the tool nose are significantly larger than those at the lower edge of the trailing edge, so the stress is mainly under the front blade edge. From the equivalent stress diagram traced in the longitudinal point of Fig.5(d), it can be seen that the maximum equivalent stress occurs at two points P3 and P5, and the P2 and P1 points at the flare surface and the P4 point at the bottom of the groove are also very stressful. From the above analysis, it can be seen that the flaring plane and the bottom of the tank are highly deformed and are the main force areas. The front blade edge and the two side edges are the major danger zones for the chipping. Therefore, the front blade, the two side blades, and the rake face (bright side) are the main parts, and the performance requirements are high.

### 3.3 Equivalent Strain Distribution

Objects are affected by external factors such as force, temperature field changes, etc. In the case of deformation in these situations, the degree of deformation in each part of the object and at each point is generally not the same. Then, when the object appears this kind of situation, we describe the object as a point of deformation within the object, in order to explain the mechanical variable of the degree of deformation at that point, that is, the strain within a point of the object. Due to the above analysis, we can find a unit at this point in the deformed object to compare the size and shape of the unit before and after the deformation. That is, the strain is the local relative deformation of the object caused by load, temperature, humidity and other factors.

The volume of the metal material remains unchanged before and after plastic deformation. According to the volume-invariant rule, when plastically deformed, only the shape and size change, but no volume change. When the metal is plastically deformed regardless of the

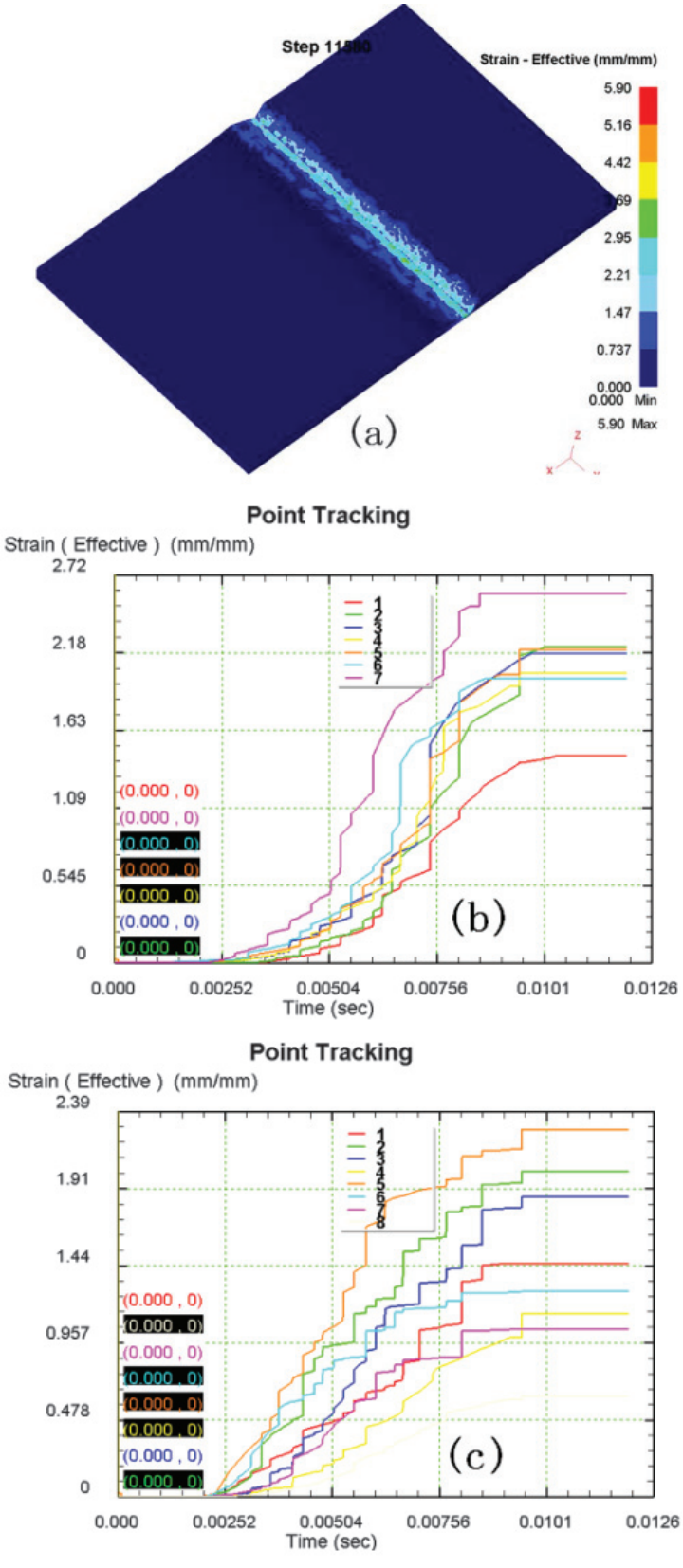


Fig.6 Equivalent strain diagram

(a) Strain cloud (b) Lateral point tracking strain diagram (c) Longitudinal point tracking strain diagram

strain state, there must be a sign of the principal strain that is opposite to the sign of the other two principal strains, and the absolute value of this principal strain is the largest.

From the equivalent strain cloud diagram in Fig. 6(a), it can be seen that in the early stage of deformation, the plastic strain of the metal mainly concentrates on the flaring surface and non-flare surface.The deformation is mainly limited to the contact area between the material and the tool, and the strain distribution increases as the squeezing process progresses, and the equivalent strain value also increases, but only in the groove shape, and the groove external equivalent strain value is small.

From Fig. 6(b) tracing the equivalent strain diagram in the transverse point, it can be seen that the maximum equivalent strain occurs at the point P7 below the front blade, and the strain values at points P2 and P5 are also large, so the main force regions are distributed in the blade. From the longitudinal point tracking equivalent strain diagram in Fig.6(c), it can be seen that the maximum equivalent strain occurs at the P5 point at the bottom of the groove, and the equivalent strain values at the two points P2 and P3 on the flare surface are also large. From the above analysis, it can be seen that the bottom of the groove and the flaring plane are the main deformation areas, and the force is relatively large. When designing the tool, the wear of the front blade and the rake face (bright side) is mainly considered.

## 4. Conclusion

Before the official marking of the knife, it must be tested. The process of test scribing mainly determines the size of the blaze angle according to the blazed wavelength of the blazed grating. In general, the blaze angle needs to be achieved by adjusting the angle of the diamond tool. By measuring the diffraction efficiency of the groove and grating of the grating, determine if the requirements have been met.Before the grating is officially scribed, there should be enough time to balance the temperature and make the machine reach a dynamic stable equilibrium. In the plastic forming process, as far as possible to create favorable deformation conditions, give full play to the metal's plasticity, reduce its deformation resistance, in order to achieve the purpose of high-quality slot shape.


## Acknowledgements

This research is supported by the special research project of basic scientific research in Heilongjiang Education Department (135209307).


## References


1. Tamir T., Wang H. C., and Oliner A. A. (2012): Wave propagation in sinusoidally stratified dielectric media. *IEEE Trans. Microwave Theory Tech*., 12(4), 323-335.
2. Li Lifeng. (2013): A modal analysis of lamellar diffraction gratings in conical mountings. *Opt. Acta*, 40(4), 553-573.
3. Li Lifeng. (2015): Note on the S-matrix propagation algorithm. J. Opt. Soc. Am., 20(4), 655-660.
4. Moharam M. G., and Gaylord T. K. (2011): Coupled-wave analysis of reflection gratings. Appl. Phys., 20(2), 240-244.
5. Moharam M. G., Pomment D. A., and Grann E. B. (2015): Stable implementation of the rigorous coupled-wave analysis for surface-relief gratings: enhanced transmittance matrix approach. *J. Opt. Soc. Am*., 12(5), 1077- 1086.
6. Grann E. B., and Moharam M. G.. (2016): Comparison between continuous and discrete subwavelength gratings structures for antireflection surfaces. *J. Opt. Soc. Am.*, 13(5), 988-992
7. Li Lifeng, Chandezon J., Granet G., and Plumey Jean-Pierre. (2009): Rigorous and efficient rating-analysis method made easy for optical engineers. *Appl Opt*, 38(2): 304-313.
8. Tremain D. E., and Mei K. K. (2008): Application of the unimoment method to scattering from periodic dielectric structures, *J. Opt. Soc. Am,* 68(6), 775-783.
9. Maystre D. (2008): A new general integral theory for dielectric coated gratings, *J. Opt. Soc. Am.*, 68(4), 490-495.
10. Hage man L J. (2007): Automative adaptive remenshing in ALPID, an advanced forging simulation program. *Comput. Eng,* 2:93-97
11. Nicolas V T, and Citipitioglu E. (2013): A general isopametric finite element program SDRC SUPERB. *Comput. Struct,* 55(7), 303-313.
12. Cheng J. (2013): Automatic adaptive remeshing for finite element simulation of forming processes. *Int. J. Num Meth. Engng*, 26(8), 1-18.